

Review

# Engineering the Interface between Inorganic Nanoparticles and Biological Systems through Ligand Design

Rui Huang , David C. Luther , Xianzhi Zhang , Aarohi Gupta , Samantha A. Tufts  
and Vincent M. Rotello \* 

Department of Chemistry, University of Massachusetts Amherst, 710 N. Pleasant St., Amherst, MA 01003, USA; ruihuang@umass.edu (R.H.); dluther@umass.edu (D.C.L.); xianzhizhang@umass.edu (X.Z.); aarohigupta@umass.edu (A.G.); satufts@umass.edu (S.A.T.)

\* Correspondence: rotello@chem.umass.edu

**Abstract:** Nanoparticles (NPs) provide multipurpose platforms for a wide range of biological applications. These applications are enabled through molecular design of surface coverages, modulating NP interactions with biosystems. In this review, we highlight approaches to functionalize nanoparticles with “small” organic ligands ( $M_w < 1000$ ), providing insight into how organic synthesis can be used to engineer NPs for nanobiology and nanomedicine.

**Keywords:** inorganic nanoparticles; surface chemistry; peptide and proteins; monolayers; nanozyme; bioorthogonal catalysis; bacterial biofilm; tumors; stimuli-responsive; drug delivery



**Citation:** Huang, R.; Luther, D.C.; Zhang, X.; Gupta, A.; Tufts, S.A.; Rotello, V.M. Engineering the Interface between Inorganic Nanoparticles and Biological Systems through Ligand Design. *Nanomaterials* **2021**, *11*, 1001. <https://doi.org/10.3390/nano11041001>

Academic Editor: Magdalena Oćwieja

Received: 17 March 2021

Accepted: 8 April 2021

Published: 13 April 2021

**Publisher's Note:** MDPI stays neutral with regard to jurisdictional claims in published maps and institutional affiliations.



**Copyright:** © 2021 by the authors. Licensee MDPI, Basel, Switzerland. This article is an open access article distributed under the terms and conditions of the Creative Commons Attribution (CC BY) license (<https://creativecommons.org/licenses/by/4.0/>).

## 1. Introduction

Inorganic nanoparticles can be engineered to possess useful physiochemical properties for use in applications including biomedicine and diagnostics [1–6]. While shape [7] and size [8] both play critical roles in defining nanoparticle properties, surface chemistry is likewise crucial for function and colloidal stability [9,10]. The nanoparticle surface interfaces with the external environment, and appropriately engineered surfaces can be used to regulate interactions between nanoparticles and biomolecules [11] including peptides [12], proteins [13] and nucleic acids [14].

A wide range of strategies have been used to modulate surface properties of nanoparticles (NPs), including polymer-based surface modification of nanoparticles [15–18]. These systems are quite useful; however, the intricacies of polymer structure and dynamics introduce complexities that add an additional layer to understanding and harnessing the interactions between nanoparticles and biomolecules [19]. Designing small ligand molecules to tailor the surface properties of nanoparticles provides an approach complementary to polymer coatings, providing ease of fabrication and scalability [20]. The wide range of functionalities provided by organic chemistry renders a rich toolkit, allowing for atom-by-atom control of nano–bio interactions contiguous [1]. In this review we provide an overview of approaches for controlling nanoparticle–cell and nanoparticle–protein interactions by tailoring small molecule ligands on the particle surface. Particle–protein interactions are important in their own right and also serve to modulate nanoparticle–cell interactions through corona formation. Nanoparticle interaction with nucleic acids [21] and intracellular delivery of nanoparticle-bound biomolecules [22] are likewise important related concepts that are beyond the scope of this review.

## 2. Modulating Nano–Bio Interactions through Surface Design

Engineered NPs can feature a diverse range of chemical surface functionalities to promote specific or nonspecific interaction with proteins or other biomolecules of interest. Proteins are particularly interesting targets for their roles in cellular homeostasis and

metabolic diseases [23,24]. Enzymatic activity is closely linked to protein structure, creating an intriguing engineering challenge for NP design at the ligand–protein interface.

### 2.1. Regulation of Enzyme Activity

NPs can be used as enzyme inhibitors by engineering them to noncovalently interact with protein surfaces, blocking access to the active site or triggering protein denaturation [25,26]. In early studies, the Rotello group functionalized gold nanoparticles (AuNPs) with COO-surface moieties to allow them to interact with the cationic region surrounding the active site of chymotrypsin, thereby inhibiting enzymatic activity [27]. Using these surfactant-like ligands, an almost complete denaturation of chymotrypsin was observed by circular dichroism (CD) upon addition of AuNPs. Importantly, negatively charged AuNPs showed a relatively high degree of selectivity to chymotrypsin over proteins like elastase and  $\beta$ -galactosidase due to electrostatic complementarity. Follow-up studies [28] demonstrated that this AuNP-based inhibition of chymotrypsin could be reversed (up to 50%) through in situ surface modification of AuNPs using long-chain surfactant (Figure 1). In related work, Hamad–Schifferli engineered a series of 9.6-nm AuNPs featuring anionic and zwitterionic functionalities to investigate the effect of surface charge on the enzymatic activity of glucose oxidase (GOx) [29]. The authors reported that neutral and zwitterionic ligands acted as a steric barrier to the active site, and further that changing AuNP surface chemistry varied binding kinetics greatly, with certain surface chemistries irreversibly affecting GOx denaturation and activity.

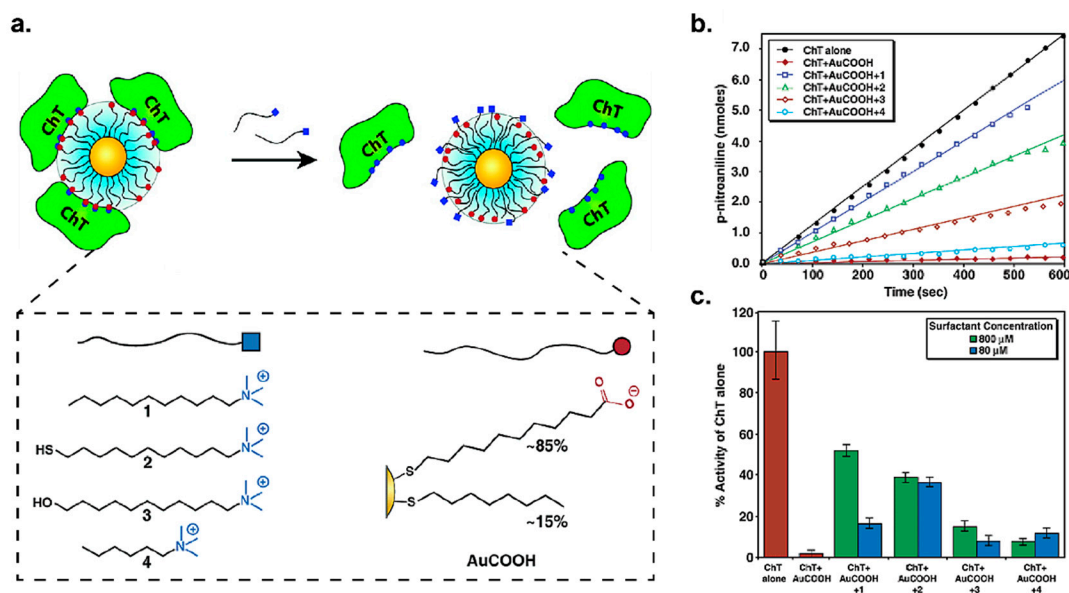


**Figure 1.** (a) Schematic illustration of the mechanism of rescuing chymotrypsin activity using long-chain surfactants. (b) Initial velocities of chymotrypsin before and after adding four different surfactants. Chymotrypsin reactivation was monitored via the hydrolysis of the chromogenic substrate *N*-succinyl-L-phenylalanine p-nitroanilide (SPNA), as measured by UV–vis spectroscopy. (c) Reactivation of chymotrypsin is dependent on surfactant concentration. (Adapted with permission from Reference [28]; Published by American Chemical Society, 2003).

Rotello showed that the nature of NP–protein interaction can be tuned using CdSe NPs featuring oligo (ethylene glycol) (OEG) ligands with chain-end functionality [30]. By varying ligand composition, the authors showed tunable surface recognition of chymotrypsin, with three levels of interaction: no interaction, inhibition with denaturation, and reversible inhibition with retention of structure. This work demonstrated NPs as versatile platforms for enzyme binding and controlled inhibition.

Amino acids functionalities are attractive candidates as NP surface moieties for enzyme inhibition as they can not only provide structural diversity but also mimic naturally occurring protein–protein interactions [31]. Rotello and coworkers generated a series of

L-amino acid-functionalized AuNPs with varied hydrophobicity and electrostatic charge to probe binding with the surface of chymotrypsin [32]. Determined by binding constant, the authors reported that AuNPs featuring hydrophobic groups bound more strongly than those with hydrophilic groups. Later work demonstrated that chirality plays a similarly important role in protein binding, and that unlike small molecule regulators, specific binding interactions significantly affect AuNP-based enzyme regulation [33].

NPs can also be functionalized with small molecule recognition elements to promote specific binding to a protein of interest for inhibition [34]. Recent work by Lira demonstrated AuNPs decorated with p-mercaptobenzoic acid ligands could bind distinct allosteric exosites of the serine protease thrombin, providing allosteric regulation of the enzyme active site without large-scale denaturation [35].

In contrast to enzyme inhibition, AuNPs can also be engineered to refold denatured enzymatic proteins. AuNPs bearing dicarboxylate functionalities promoted the refolding of thermally denatured cationic enzymes, including chymotrypsin, lysozyme and papain to their native conformations [36]. The Vinogradov group reported alumina NPs as agents to promote renaturation of misfolded enzymes with overall anionic charge [37]. More recently, Khare demonstrated magnetic iron oxide nanoparticles featuring aminopropyl triethoxysilane (APTES) modifications that were capable of refolding thermally denatured enzymes [38]. After incubation between APTES-NPs and thermally denatured cholesterol oxidases, dynamic light scattering (DLS), zeta potential measurements, fluorescence and CD spectroscopy confirmed enzyme refolding to the native state. Similar engineering approaches could provide an avenue for specific enzyme regulation for therapeutic purposes, including refolding of misfolded enzymes linked to diseases.

## 2.2. Modulating Interactions between NPs and Proteins

Nanoparticles administered into the blood can interact nonspecifically with serum proteins and form a shell of protein, called the protein corona [39–44]. Protein corona formation is mainly mediated by coulombic and Van der Waals forces, hydrogen bonding, and hydrophobic interactions [45]. Moreover, the wetting behavior of the NP surface also plays an important role in regulating protein adhesion behaviors [46–48]. Protein corona provides new “identity” to nanomaterials in the biological environment, significantly affecting NPs in terms of their biodistribution, cellular uptake and cargo release [49–51]. Moreover, the protein corona diminishes targeting effects of NPs and accelerates their clearance from the body through the mononuclear phagocyte system (MPS), greatly hampering therapeutic potential for nanomedicines [52]. Tuning the hydrophilicity and electroneutrality of the NP monolayer provides an effective way to reduce protein absorption on the surface [53].

OEG has been widely used to functionalize NP surfaces to reduce protein corona formation [54–57]. The terminal hydroxyl group provides little to no charge to the entire system, while the ethylene glycol units provide hydrophilicity. Work by Rotello reported that AuNPs functionalized with thioalkylated OEG showed minimized protein adsorption [58]. Walker and coworkers similarly demonstrated the creation of nonfouling AuNPs using OEG groups [59]. Interestingly, rate constant of protein–AuNP dissociation was quantified by introducing nonequilibrium capillary electrophoresis of equilibrium mixtures (NECEEM) in this work. Recently, Gentili [60] reported that the use of OEG-alkanethiol on silver nanoparticles efficiently reduced corona formation in serum-containing media, as confirmed by UV–vis spectroscopy, DLS and zeta potential (Figure 2).

Incorporating zwitterionic functionalities such as amino acids onto the NP surface is an alternative to the use of OEG [61,62]. Early work by Frangioni demonstrated that functionalizing quantum dots with cysteine and tumor targeting moieties could reduce corona formation and provide “stealth” character while enhancing targeting efficiency [63]. More recently, a similar strategy was adopted to modify the surface of fluorescent silica nanoparticles (SiNPs) by Mahmoudi’s group [64]. In this study biotin was used as a ligand to target tumor cells bearing biotin receptors, with zwitterionic cysteine incorporated to avoid formation of the protein corona, as confirmed by gel electrophoresis. Studies

with several cell lines, two biotin receptor-positive and another receptor-negative, demonstrated that nonfouling SiNPs have significantly improved targeting efficiency compared to counterparts modified with cysteine or biotin only.

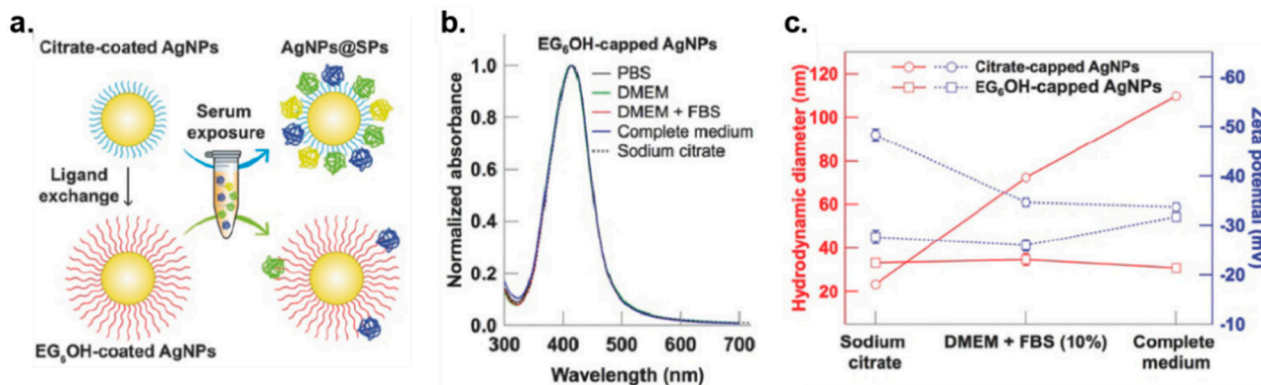


**Figure 2.** (a) Schematic illustration of serum protein adsorption on the surface of citrate-coated AgNPs and the formation of nonfouling AgNPs by coating OEG groups. (b) The stability of OEG-functionalized AgNPs was confirmed by measuring UV-vis absorption spectra in various culture medium. (c) Hydrodynamic diameter and zeta potential of AgNPs before and after incubation in growth media. (Adapted with permission from Reference [60]; Published by WILEY, 2018).

In addition to amino acids, zwitterionic betaine groups have also been widely used for functionalization to enhance NP stealth properties [65]. Rotello developed AuNPs with a series of sulfobetaine terminal groups of variable hydrophobicity, reporting no protein adsorption at physiological serum concentrations [66]. Later work by Parak and coworkers reported that quantum dots coated with sulfobetaine ligands showed negligible change in size after incubating with human serum albumin, suggesting no corona formation [67]. Recently, betaine-based zwitterionic AuNPs [68] were used by Rotello to encapsulate transition metal catalysts (TMCs) within the ligand monolayer to obtain bioorthogonal nanoenzymes, or “nanozymes” (NZs) (Figure 3). Bioorthogonal NZs are artificial enzymes that can generate imaging or therapeutic agents in situ in biological systems through bond cleavage reactions [69–72]. Kinetic studies showed that NZs functionalized with zwitterionic surface functionalities maintain high catalytic activity in biological environments due to their “corona-free” properties [73–75].

### 2.3. Modulating NP-Cell Interactions

Cells interact with NPs mainly through Van der Waals and electrostatic interactions. These noncovalent interactions can be modulated through tuning NP physicochemical properties such as charge and hydrophobicity [76].

Surface charge of NPs plays an important role in their cellular uptake [77–79]. Typically, anionic and neutral NPs have low affinity for the anionic cell membrane whereas cationic NPs are strongly electrostatically attracted to the membrane (Figure 4).

Based on this electrostatic property, a wide range of NPs have been engineered to carry positive charge for their enhanced cellular internalization [80–87]. Additionally, surface charge modification can also be used to dictate either extra- or intracellular localization of NPs [75]. Rotello noncovalently incorporated dyes or drugs into zwitterionic AuNPs for enhanced delivery efficiency [82]. As demonstrated by fluorescence microscopy and cytotoxicity assays, encapsulated drugs or dyes were efficiently released into cells. Importantly, there is little or no cellular uptake of AuNPs due to the noninteracting nature of their surfaces with cells, as confirmed by transmission electron microscopy (TEM) and inductively coupled plasma mass spectrometry (ICP–MS). Recently, these zwitterionic AuNPs were used to encapsulate TMCs to localize the catalyst molecules specifically to the extracellular region [75]. As shown in Figure 5, the spatial control of bioorthogonal catalysis can be achieved by using positive or zwitterionic surfaces.

NP hydrophobicity is another key parameter that affects cellular uptake [88,89]. Guével demonstrated that cationic gold nanoclusters with increasing surface hydrophobicity showed concomitantly enhanced cellular internalization [90]. Similarly, Zheng introduced hydrophobic octanethiol onto the surface of zwitterionic AuNPs to enhance their affinity for the cell membrane and observed an enhancement in cellular uptake by more than an order of magnitude [91].

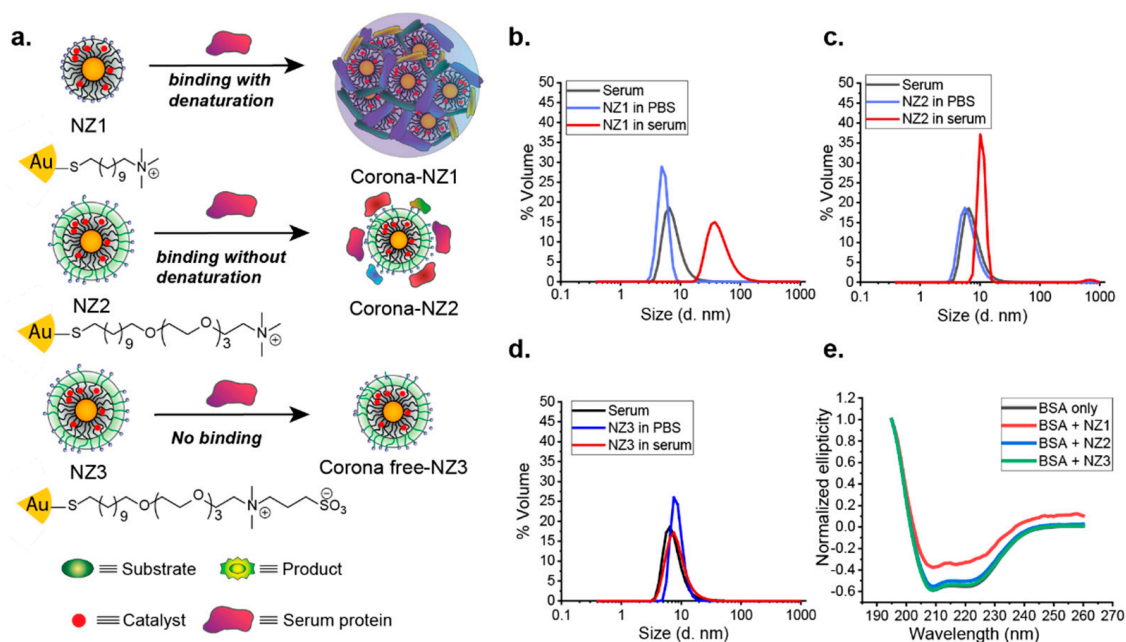


**Figure 3.** (a) Schematic illustration of tuning ligand monolayers to modulate interactions between AuNPs and proteins. As confirmed by dynamic light scattering (DLS) (b–d), nanozyme-2 (NZ2) formed a corona-like structure with serum proteins while NZ1 formed aggregates. Zwitterionic NZ3 showed nonfouling property in the presence of serum medium. (e) Circular dichroism (CD) results demonstrated that NZ1 partially denatured bovine serum albumin (BSA), inducing its conformational changes. However, NZ2 and NZ3 retained the original protein conformation. (Adapted with permission from Reference [68]; Published by American Chemical Society, 2020).

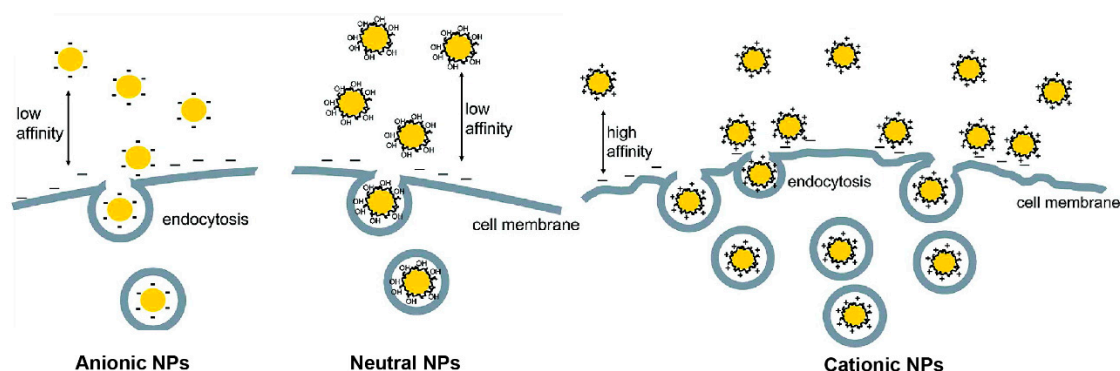


**Figure 4.** Schematic illustration of the interactions between NPs with different types of surface charges and cells. (Adapted with permission from Reference [77]; Published by American Chemical Society, 2009).

Active targeting is a strategy to provide enhanced cellular uptake by utilizing affinity ligands on the NP surface for specific recognition with receptors overexpressed on target cells [92,93]. Small molecule ligands (e.g., folic acid, methotrexate, anisamide, cholic acid, daptomycin, fluorine and sugars) have been utilized extensively for conjugation to various inorganic NPs due to their stability, ease of modification and availability [94–96]. To date, several therapeutic and diagnostic approaches using active targeting NPs have entered clinical trials, with several gaining FDA approval [97].

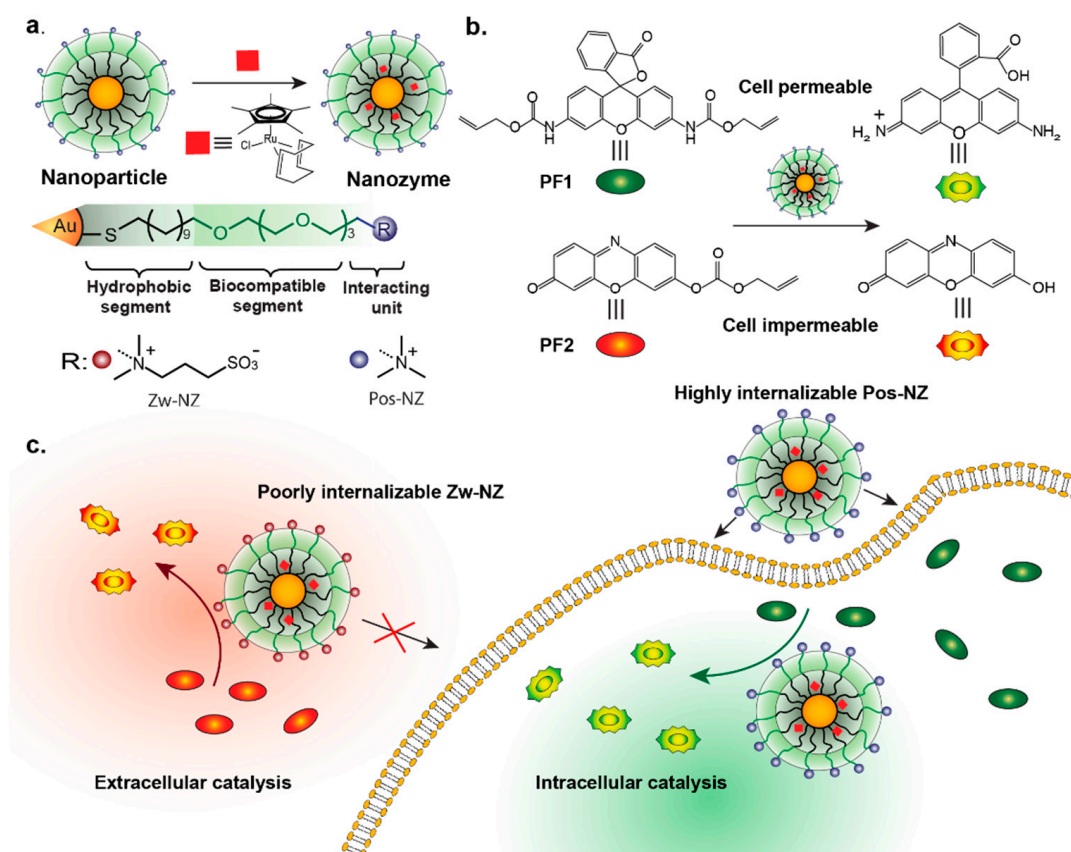


**Figure 5.** (a) Schematic representation of nanoparticles, nanozymes and ligand structures of zwitterionic nanozymes (Zw-NZ) and cationic nanozymes (Pos-NZ). (b) Structures of prodyes and their corresponding fluorescent products (rhodamine 110 and resorufin) after bond cleavage catalyzed by Ru-based complex in NZs. (c) Schematic representation of specific localization of nanozymes by engineering surface functionalities; activation of PF1 happens in intracellular region while that of PF2 occurs extracellularly. (Adapted with permission from Reference [75], Published by American Chemical Society, 2019).

Folic acid (FA) is a frequently used targeting moiety due to overexpression of the folate receptor on cancerous cells and inflamed tissue [98–103]. In work by Zhang, superparamagnetic iron oxide nanoparticles were modified with methotrexate (MTX), a small-molecule chemotherapeutic and synthetic analog of FA [104]. These NPs exhibited enhanced uptake in MCF-7 and HeLa cancer cells, with enhanced cancer cell death after MTX release triggered by low lysosomal pH (Figure 6). Similar approaches have recently seen success using AuNPs [105] and mesoporous silica [106]. Benzamides are another commonly used class of active targeting ligand for their ability to target the sigma receptors overexpressed on prostate cancer cells [107,108]. Anisamide variants have been conjugated to poly(ethyleneamine) (PEI) gold nanospheres [109] or PEGylated AuNPs [110] to facilitate cell-specific internalization of siRNA-conjugated AuNPs, both in vitro and in vivo. Similar approaches have utilized NP conjugation of biotin [111], mannose [112,113] or hyaluronic acid (HA) [114,115] for targeted delivery to various cell types.

Chan examined the effect of diameter on tumor uptake of spherical AuNPs, with and without targeting ligand (transferrin coating). The authors reported no significant differences with particles  $\leq 100$  nm, but observed tumor accumulation five times faster and two-fold higher with targeted, transferrin-coated particles [100,116]. Later work from this laboratory critically examined tumor targeting by showing that less than 14 out of 1 million (0.0014% injected dose) intravenously administered targeted NPs were delivered to targeted cancer cells, with the majority trapped in the extracellular matrix or phagocytosed by macrophages [117]. This work helped to show that a re-examining of the active targeting process is necessary for translation of NP therapeutics, and that interaction between NPs and cells is significantly more complicated when moved in vivo.

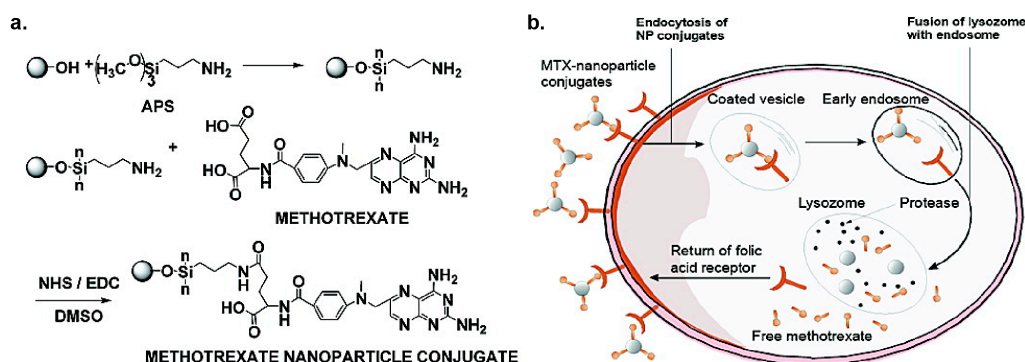


**Figure 6.** (a) Surface modification of magnetite nanoparticles with methotrexate (MTX). (b) Schematic representation of MTX release in simulated lysosomal pH conditions. (Adapted with permission from Reference [104]; Published by American Chemical Society, 2005).

### 3. Modulating Nano-Bio Interactions through Stimuli-Responsive NPs

NP localization at both the organismal and cell level remains a challenge to nanotherapeutics. Engineering NPs for stimuli responsiveness is an effective strategy to enhance NP localization at a desired locale [118,119]. Versatile NP ligands can be designed to respond to optical stimuli, pH differences and enzyme-induced cleavage.

#### 3.1. Enzyme-Induced Aggregate Formation

Efficient cellular uptake is crucial for nanoparticle use in bioapplications, including diagnosis and therapy [77,88]. Stimuli-responsive aggregation has been widely used as a way to enhance accumulation of NPs in cells [120]. Once AuNPs aggregate inside cells, exocytosis will be blocked and their backflow to the bloodstream will be restricted, effectively enhancing cellular retention of AuNPs [121]. Gao created a nanoscale platform consisting of AuNPs functionalized with peptides (Ala-Ala-Asn-Cys-Lys) (AuNPs-AK) and AuNPs grafted with 2-cyano-6-amino-benzothiazole (AuNPs-CABT) to trigger intracellular aggregation [122]. With this system, peptide-modified AuNPs undergo ligand hydrolysis in the presence of the proteolytic enzyme legumain, which triggers the formation of aggregates due to a click cycloaddition reaction between the newly formed 1,2-thiolamino moiety and the contiguous cyano group (Figure 7). Later studies in murine glioma models showed that this AuNP-based nanoplatform was able to aggregate rapidly upon entering into glioma cells, resulting in an increased amount of AuNPs internalized and greater tumor cell death when compared to nonaggregated counterparts. Later work from this group introduced new elements to the AuNP ligands to improve their membrane permeability and target different tumor models. Octaarginine and arginylglycylaspartic acid [123] were simultaneously conjugated to the ligand for an enhanced AuNP accumulation in glioblastoma cells while cediranib [124] was grafted for that in 4T1 cells.

#### 3.2. pH-Dependent Aggregate Formation

Another common stimulus to trigger nanoparticle aggregation is pH, a property can be used to target acidic microenvironments such as those found in tumors or bacterial biofilms [125–128]. Early work by Kim demonstrated that nanoparticles can respond to pH changes and form aggregates [129]. Hydrolysis-susceptible citraconic amide was used to functionalize AuNPs for its ability to undergo partial bond cleavage at a pH lower than 7, forming positively charged primary amines. Upon hydrolysis, the surface charge is neutralized and AuNPs begins to aggregate in the absence of electrostatic repulsion. Compared to counterparts with permanent negative charge, pH-responsive AuNPs demonstrated enhanced cellular uptake in B16F10 and NIH 3T3 cells, confirmed by dark field optical microscopy. This platform was later used for photoacoustic imaging [130] and showed a cancer-specific AuNP accumulation at the cellular level (Figure 8a). Inspired by the Kim group, Wong and coworkers functionalized AuNPs with a hydrolysis-susceptible citraconic

amide moiety for pH-responsiveness and a peptide for active tumor-targeting ability [131]. Engineered AuNPs demonstrated efficient cellular uptake in U-87MG cells both in vitro and in vivo.

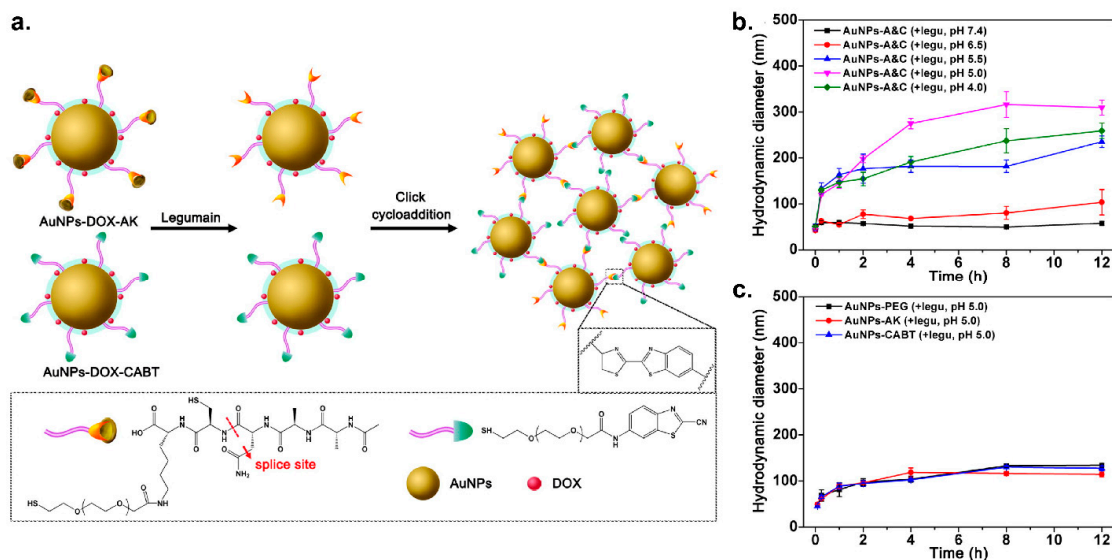


**Figure 7.** (a) Schematic representation of the legumain-triggered AuNP aggregation and composition of AuNPs functionalized with peptides (Ala-Ala-Asn-Cys-Lys) (AuNPs-AK) and AuNPs grafted with 2-cyano-6-amino-benzothiazole (AuNPs-CABT). (b) The proteolytic capacity of legumain is pH dependent. As a result, AuNP aggregation triggered by legumain varied at different pH values and the size increase was the highest at pH 5.0, as confirmed by DLS measurement. (c) AuNPs functionalized with PEG, AuNPs-AK only or AuNPs-CABT only was used as controls. DLS data showed that no aggregation was observed when treated with legumain at pH 5.0. (Adapted with permission from Reference [122], Published by American Chemical Society, 2016).

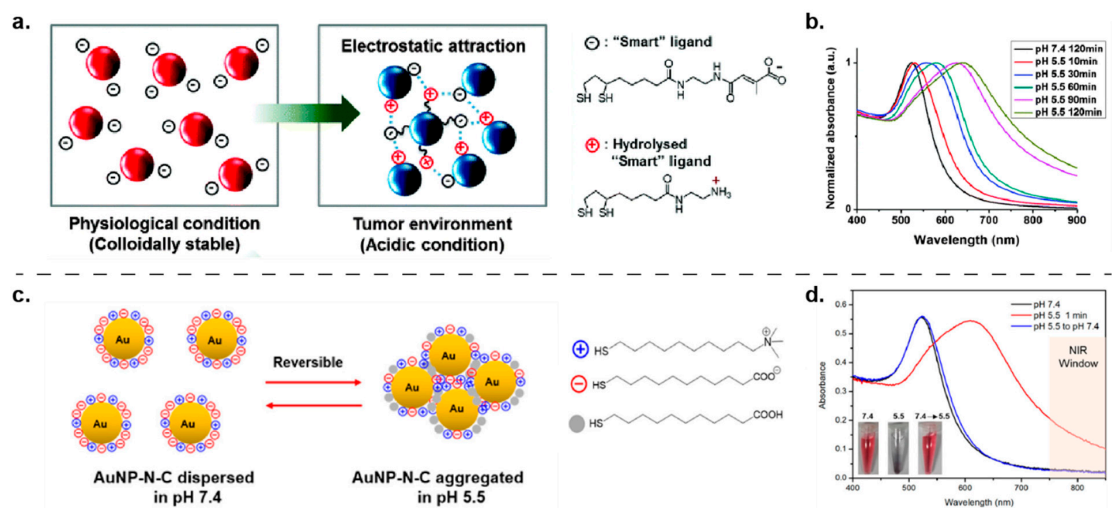


**Figure 8.** Schematic representation of pH-triggered AuNP aggregation through two different mechanisms. (a) The surface charge of AuNPs is designed to switch from negative to a mixture of negative and positive charges through bond cleavage under the mildly acidic conditions; once the surface charge is neutralized, AuNPs begin to aggregate due to the absence of electrostatic repulsion. (Adapted with permission from Reference [130]; Published by Royal Society of Chemistry, 2016). This transformation was monitored by (b) UV-vis spectroscopy for 2 h. (c) The surface charge of AuNPs is designed to be neutralized owing to the protonation of MUA ligand under the mildly acidic conditions. As demonstrated by UV-vis spectroscopy (d), this transformation is reversible. (Adapted with permission from Reference [132]; Published by American Chemical Society, 2017).

In addition to pH-induced bond cleavage, pH-dependent protonation/deprotonation transition has also been used as a strategy for surface neutralization to trigger aggregation of nanoparticles. Grzybowski and coworkers developed a series of zwitterionic AuNPs using both *N,N,N*-trimethyl(11-mercaptoundecyl)ammonium ion (TMA) and 11-mercaptoundecanoic acid (MUA) as ligands for surface modification [133]. The protonation of the MUA ligand at low pH can neutralize the surface charge of AuNPs to form aggregates through Van der Waals attractions and hydrogen bonding. Importantly, the precipitating pH value of these zwitterionic AuNPs can be engineered by tuning MUA/TMA ratio, providing an avenue for pH-specific biological targeting. Using a similar approach, Ji fabricated a series of pH-responsive zwitterionic AuNPs for tumor treatment [134]. It was observed that optimized AuNPs were stable at the pH of blood and normal tissues but aggregated rapidly in response to acidic tumor environment, rendering a significantly enhanced cellular internalization of particles compared to nonsensitive PEGylated AuNP controls. More recently, this platform was used to treat methicillin-resistant *Staphylococcus aureus* (MRSA) bacterial biofilm (Figure 8c). In animal studies, the aggregation of AuNPs triggered by acidic biofilm microenvironment facilitated localization in the biofilm extracellular polymeric substance (EPS), allowing for effective NIR photochemical therapy with minimal toxicity to normal healthy cells [132]. To further develop this system, Li performed coarse-grained (CG) molecular dynamics simulations to systematically investigate the stability of MUA/TMA-based pH-responsive AuNPs and their interactions with cells [135].

### 3.3. pH-Responsive Charge Conversion

As mentioned previously, cationic nanoparticles generally display significantly higher cellular internalization compared to zwitterionic counterparts due to electrostatic attraction with the negatively charged cell membrane [78,79]. Based on this property, the Rotello group functionalized AuNPs with a pH-responsive sulfonamide-based ligand of which the surface charge can switch from zwitterionic to cationic at mildly acidic conditions to enhance cellular uptake in the acidic tumor microenvironment [136]. ICP-MS data showed that cellular uptake of AuNPs at pH 6.0 was four-fold higher than that at pH 7.4 and no aggregation was observed under any conditions, as confirmed by DLS. Recently, the You group utilized a similar sulfonamide-based ligand to modify the surface of their gold nanocages [137]. After intravenous injection into 4T1 murine breast tumor models, pH-responsive AuNPs exhibited efficient accumulation within tumor cells.

Similar approaches have been taken to target the acidic microenvironment of bacterial biofilm infections. In 2018, Rotello group investigated the interaction of pH-responsive AuNPs featuring sulfonamide moieties with bacterial biofilms [138]. Zwitterionic AuNPs transitioned to cationic at the acidic biofilm pH, essentially “honing” to the infection due to strong electrostatic interaction (Figure 9). In a fibroblast–biofilm coculture model, AuNPs selectively penetrated and accumulated inside biofilms. In an alternative approach, carboxyl betaines were recently used by Luo to modify the surface of silver nanoparticles, resulting in enhanced adhesion of nanoparticles to the bacteria membrane [139].

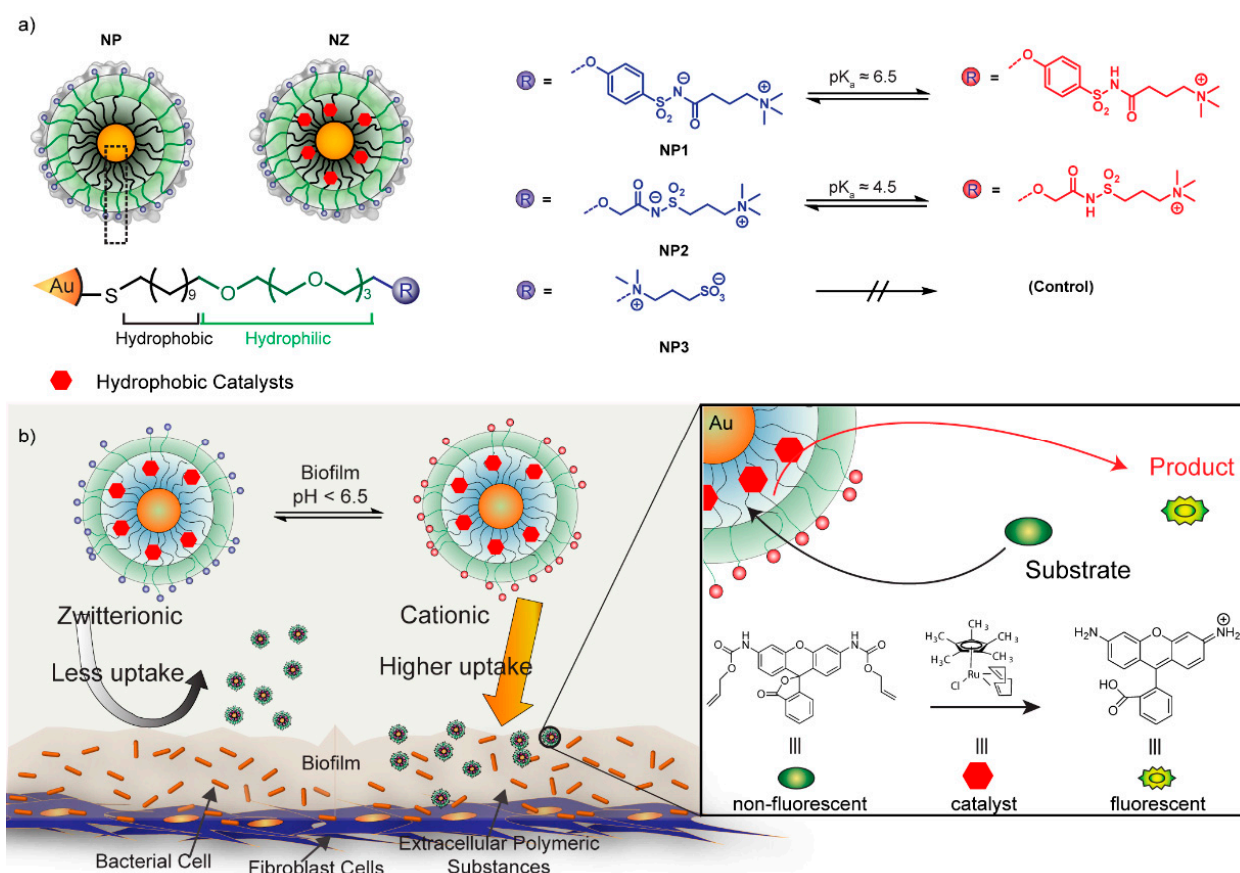


**Figure 9.** (a) Schematic representation of nanoparticles, nanozymes and molecular structures of pH-switchable and control ligands on AuNPs. (b) Schematic representation showing selective targeting of biofilm infections using pH-responsive nanoparticles and NZ-mediated fluorogenesis of prodye inside of biofilms. (Adapted with permission from Reference [138]; Published by American Chemical Society, 2018).

#### 4. Conclusions

As demonstrated in this review, engineered NP surface chemistry provides a powerful avenue to tailor the physicochemical properties of NPs, offering potential to surpass obstacles and enhance efficiency in nanomedicine. The examples highlighted herein demonstrate the power of NP surface functionalization to control nano–bio interactions, from modulation of enzymatic activity to selective localization in specific cell types. Nanomaterials undergo complex interactions with biomolecules and cell surfaces, and the chemical versatility granted by NP ligands thus remains an unmatched tool in exploring the nano–bio interface.

Organic chemistry provides an immense range of chemical diversity for the functionalization of NPs. The breadth of chemical functionalities available provides a rich toolkit to probe nano–bio interactions. Future research will continue to move toward precise control over biochemical interactions and provide a deeper understanding of structure–function relationships. Such studies will further extend the potential of NP platforms in therapeutics, imaging and diagnostics.

**Author Contributions:** Conceptualization, R.H., D.C.L. and V.M.R.; writing—original draft preparation, R.H., D.C.L., X.Z., A.G., S.A.T.; writing—review and editing, R.H., D.C.L., V.M.R.; supervision, V.M.R.; project administration, V.M.R.; funding acquisition, V.M.R.; All authors have read and agreed to the published version of the manuscript.

**Funding:** This research was funded by the National Institutes of Health (DK121351, AI134770 and EB022641).

**Conflicts of Interest:** The authors declare no conflict of interest.

## References

1. Nienhaus, K.; Wang, H.; Nienhaus, G. Nanoparticles for biomedical applications: Exploring and exploiting molecular interactions at the nano-bio interface. *Mater. Today Adv.* **2020**, *5*, 100036. [[CrossRef](#)]
2. Kulu, I.; Huang, R.; Kalyanaraman, B.; Rotello, V.M. A modified and simplified method for purification of gold nanoparticles. *MethodsX* **2020**, *7*, 100896. [[CrossRef](#)]
3. Luther, D.C.; Huang, R.; Jeon, T.; Zhang, X.; Lee, Y.-W.; Nagaraj, H.; Rotello, V.M. Delivery of drugs, proteins, and nucleic acids using inorganic nanoparticles. *Adv. Drug Deliv. Rev.* **2020**, *156*, 188–213. [[CrossRef](#)]
4. Kango, S.; Kalia, S.; Celli, A.; Njuguna, J.; Habibi, Y.; Kumar, R. Surface Modification of Inorganic Nanoparticles for Development of Organic–Inorganic Nanocomposites—A Review. *Prog. Polym. Sci.* **2013**, *38*, 1232–1261. [[CrossRef](#)]
5. Roy, S.; Liu, Z.; Sun, X.; Gharib, M.; Yan, H.; Huang, Y.; Megahed, S.; Schnabel, M.; Zhu, D.; Feliu, N.; et al. Assembly and Degradation of Inorganic Nanoparticles in Biological Environments. *BioConjug. Chem.* **2019**, *30*, 2751–2762. [[CrossRef](#)]
6. Retout, M.; Blond, P.; Jabin, I.; Bruylants, G. Ultrastable PEGylated Calixarene-Coated Gold Nanoparticles with a Tunable Bioconjugation Density for Biosensing Applications. *BioConjug. Chem.* **2021**, *32*, 290–300. [[CrossRef](#)]
7. Visalakshan, R.M.; García, L.E.G.; Benzigar, M.R.; Ghazaryan, A.; Simon, J.; Mierczynska-Vasilev, A.; Michl, T.D.; Vinu, A.; Mailänder, V.; Morsbach, S.; et al. The Influence of Nanoparticle Shape on Protein Corona Formation. *Small* **2020**, *16*, e2000285. [[CrossRef](#)]
8. Engstrom, A.M.; Faase, R.A.; Marquart, G.W.; Baio, J.E.; Mackiewicz, M.R.; Harper, S.L. Size-Dependent Interactions of Lipid-Coated Gold Nanoparticles: Developing a Better Mechanistic Understanding Through Model Cell Membranes and in vivo Toxicity. *Int. J. Nanomed.* **2020**, *15*, 4091–4104. [[CrossRef](#)] [[PubMed](#)]
9. Chen, D.; Ganesh, S.; Wang, W.; Amiji, M. The role of surface chemistry in serum protein corona-mediated cellular delivery and gene silencing with lipid nanoparticles. *Nanoscale* **2019**, *11*, 8760–8775. [[CrossRef](#)] [[PubMed](#)]
10. Srijampa, S.; Buddhisa, S.; Ngernpimai, S.; Leelayuwat, C.; Prongvitaya, S.; Chompoosor, A.; Tippayawat, P. Influence of Gold Nanoparticles with Different Surface Charges on Localization and Monocyte Behavior. *BioConjug. Chem.* **2020**, *31*, 1133–1143. [[CrossRef](#)] [[PubMed](#)]
11. Auría-Soro, C.; Nesma, T.; Juanes-Velasco, P.; Landeira-Viñuela, A.; Fidalgo-Gomez, H.; Acebes-Fernandez, V.; Gongora, R.; Parra, M.J.A.; Manzano-Roman, R.; Fuentes, M. Interactions of Nanoparticles and Biosystems: Microenvironment of Nanoparticles and Biomolecules in Nanomedicine. *Nanomaterials* **2019**, *9*, 1365. [[CrossRef](#)]
12. Kim, B.; Shin, J.; Wu, J.; Omstead, D.T.; Kiziltepe, T.; Littlepage, L.E.; Bilgicer, B. Engineering peptide-targeted liposomal nanoparticles optimized for improved selectivity for HER2-positive breast cancer cells to achieve enhanced in vivo efficacy. *J. Control. Release* **2020**, *322*, 530–541. [[CrossRef](#)] [[PubMed](#)]
13. Pinals, R.L.; Chio, L.; Ledesma, F.; Landry, M.P. Engineering at the nano-bio interface: Harnessing the protein corona towards nanoparticle design and function. *Analyst* **2020**, *145*, 5090–5112. [[CrossRef](#)] [[PubMed](#)]
14. Deal, B.R.; Ma, R.; Ma, V.P.-Y.; Su, H.; Kindt, J.T.; Salaita, K. Engineering DNA-Functionalized Nanostructures to Bind Nucleic Acid Targets Heteromultivalently with Enhanced Avidity. *J. Am. Chem. Soc.* **2020**, *142*, 9653–9660. [[CrossRef](#)] [[PubMed](#)]
15. Zhang, D.-X.; Yoshikawa, C.; Welch, N.G.; Pasic, P.; Thissen, H.; Voelcker, N.H. Spatially Controlled Surface Modification of Porous Silicon for Sustained Drug Delivery Applications. *Sci. Rep.* **2019**, *9*, 1–11. [[CrossRef](#)]
16. Wu, Y.; Lu, Z.; Li, Y.; Yang, J.; Zhang, X. Surface Modification of Iron Oxide-Based Magnetic Nanoparticles for Cerebral Theranostics: Application and Prospection. *Nanomaterials* **2020**, *10*, 1441. [[CrossRef](#)]
17. Thi, T.T.H.; Pilkington, E.H.; Nguyen, D.H.; Lee, J.S.; Park, K.D.; Truong, N.P. The Importance of Poly(ethylene glycol) Alternatives for Overcoming PEG Immunogenicity in Drug Delivery and Bioconjugation. *Polymers* **2020**, *12*, 298. [[CrossRef](#)]
18. Kritchenkov, I.S.; Zhukovsky, D.D.; Mohamed, A.; Korzhikov-Vlakh, V.A.; Tennikova, T.B.; Lavrentieva, A.; Scheper, T.; Pavlovskiy, V.V.; Porsev, V.V.; Evarestov, R.A.; et al. Functionalized Pt(II) and Ir(III) NIR Emitters and Their Covalent Conjugates with Polymer-Based Nanocarriers. *BioConjug. Chem.* **2020**, *31*, 1327–1343. [[CrossRef](#)]
19. Mizuhara, T.; Moyano, D.F.; Rotello, V.M. Using the power of organic synthesis for engineering the interactions of nanoparticles with biological systems. *Nano Today* **2016**, *11*, 31–40. [[CrossRef](#)]
20. Heuer-Jungemann, A.; Feliu, N.; Bakaimi, I.; Hamaly, M.; Alkilany, A.; Chakraborty, I.; Masood, A.; Casula, M.F.; Kostopoulou, A.; Oh, E.; et al. The Role of Ligands in the Chemical Synthesis and Applications of Inorganic Nanoparticles. *Chem. Rev.* **2019**, *119*, 4819–4880. [[CrossRef](#)]
21. Sokolova, V.; Epple, M. Inorganic Nanoparticles as Carriers of Nucleic Acids into Cells. *Angew. Chem. Int. Ed.* **2008**, *47*, 1382–1395. [[CrossRef](#)]
22. Reineke, T.M.; Raines, R.T.; Rotello, V.M. Delivery of Proteins and Nucleic Acids: Achievements and Challenges. *BioConjug. Chem.* **2018**, *30*, 261–262. [[CrossRef](#)] [[PubMed](#)]
23. Gonzalez, F.J.; Xie, C.; Jiang, C. The role of hypoxia-inducible factors in metabolic diseases. *Nat. Rev. Endocrinol.* **2019**, *15*, 21–32. [[CrossRef](#)]
24. Ghouri, N.; Preiss, D.; Sattar, N. Liver enzymes, nonalcoholic fatty liver disease, and incident cardiovascular disease: A narrative review and clinical perspective of prospective data. *Hepatology* **2010**, *52*, 1156–1161. [[CrossRef](#)]
25. Nakamoto, M.; Zhao, D.; Benice, O.R.; Lee, S.-H.; Shea, K.J. Abiotic Mimic of Endogenous Tissue Inhibitors of Metalloproteinases: Engineering Synthetic Polymer Nanoparticles for Use as a Broad-Spectrum Metalloproteinase Inhibitor. *J. Am. Chem. Soc.* **2020**, *142*, 2338–2345. [[CrossRef](#)]

26. Verma, A.; Simard, J.M.; Worrall, A.J.W.E.; Rotello, V.M. Tunable Reactivation of Nanoparticle-Inhibited  $\beta$ -Galactosidase by Glutathione at Intracellular Concentrations. *J. Am. Chem. Soc.* **2004**, *126*, 13987–13991. [[CrossRef](#)] [[PubMed](#)]
27. Fischer, N.O.; McIntosh, C.M.; Simard, J.M.; Rotello, V.M. Inhibition of chymotrypsin through surface binding using nanoparticle-based receptors. *Proc. Natl. Acad. Sci. USA* **2002**, *99*, 5018–5023. [[CrossRef](#)]
28. Fischer, N.O.; Verma, A.; Goodman, C.M.; Simard, J.M.; Rotello, V.M. Reversible “Irreversible” Inhibition of Chymotrypsin Using Nanoparticle Receptors. *J. Am. Chem. Soc.* **2003**, *125*, 13387–13391. [[CrossRef](#)]
29. Tellechea, E.; Wilson, K.J.; Bravo, E.; Hamad-Schifferli, K. Engineering the Interface between Glucose Oxidase and Nanoparticles. *Langmuir* **2012**, *28*, 5190–5200. [[CrossRef](#)] [[PubMed](#)]
30. Hong, R.; Fischer, N.O.; Verma, A.; Goodman, C.M.; Emrick, T.; Rotello, V.M. Control of Protein Structure and Function through Surface Recognition by Tailored Nanoparticle Scaffolds. *J. Am. Chem. Soc.* **2004**, *126*, 739–743. [[CrossRef](#)]
31. Spicer, C.D.; Jumeaux, C.; Gupta, B.; Stevens, M.M. Peptide and protein nanoparticle conjugates: Versatile platforms for biomedical applications. *Chem. Soc. Rev.* **2018**, *47*, 3574–3620. [[CrossRef](#)]
32. You, C.-C.; De, M.; Han, A.G.; Rotello, V.M. Tunable Inhibition and Denaturation of  $\alpha$ -Chymotrypsin with Amino Acid-Functionalized Gold Nanoparticles. *J. Am. Chem. Soc.* **2005**, *127*, 12873–12881. [[CrossRef](#)]
33. You, C.-C.; Agasti, S.S.; Rotello, V.M. Isomeric Control of Protein Recognition with Amino Acid- and Dipeptide-Functionalized Gold Nanoparticles. *Chem. A Eur. J.* **2007**, *14*, 143–150. [[CrossRef](#)]
34. Lira, A.L.; Ferreira, R.S.; Torquato, R.J.S.; Oliva, M.L.V.; Schuck, P.; Sousa, A.A. Allosteric inhibition of  $\alpha$ -thrombin enzymatic activity with ultrasmall gold nanoparticles. *Nanoscale Adv.* **2018**, *1*, 378–388. [[CrossRef](#)] [[PubMed](#)]
35. Lira, A.L.; Ferreira, R.S.; Oliva, M.L.V.; Sousa, A.A. Regulation of Thrombin Activity with Ultrasmall Nanoparticles: Effects of Surface Chemistry. *Langmuir* **2020**, *36*, 7991–8001. [[CrossRef](#)] [[PubMed](#)]
36. De, M.; Rotello, V.M. Synthetic “chaperones”: Nanoparticle-mediated refolding of thermally denatured proteins. *Chem. Commun.* **2008**, *30*, 3504–3506. [[CrossRef](#)]
37. Volodina, K.V.; Avnir, D.; Vinogradov, V.V. Alumina nanoparticle-assisted enzyme refolding: A versatile methodology for proteins renaturation. *Sci. Rep.* **2017**, *7*, 1458. [[CrossRef](#)]
38. Ghosh, S.; Ahmad, R.; Khare, S. Refolding of thermally denatured cholesterol oxidases by magnetic nanoparticles. *Int. J. Biol. Macromol.* **2019**, *138*, 958–965. [[CrossRef](#)]
39. Cedervall, T.; Lynch, I.; Lindman, S.; Berggård, T.; Thulin, E.; Nilsson, H.; Dawson, K.A.; Linse, S. Understanding the nanoparticle-protein corona using methods to quantify exchange rates and affinities of proteins for nanoparticles. *Proc. Natl. Acad. Sci. USA* **2007**, *104*, 2050–2055. [[CrossRef](#)]
40. Wang, H.; Dardir, K.; Lee, K.-B.; Fabris, L. Impact of Protein Corona in Nanoflare-Based Biomolecular Detection and Quantification. *BioConjug. Chem.* **2019**, *30*, 2555–2562. [[CrossRef](#)] [[PubMed](#)]
41. De Castro, C.E.; Panico, K.; Stangherlin, L.M.; Ribeiro, C.A.S.; Da Silva, M.C.C.; Carneiro-Ramos, M.S.; Dal-Bó, A.G.; Giacomelli, F.C. The Protein Corona Conundrum: Exploring the Advantages and Drawbacks of its Presence around Amphiphilic Nanoparticles. *BioConjug. Chem.* **2020**, *31*, 2638–2647. [[CrossRef](#)]
42. Docter, D.; Westmeier, D.; Markiewicz, M.; Stolte, S.; Knauer, S.K.; Stauber, R.H. The nanoparticle biomolecule corona: Lessons learned—Challenge accepted? *Chem. Soc. Rev.* **2015**, *44*, 6094–6121. [[CrossRef](#)] [[PubMed](#)]
43. Fleischer, C.C.; Payne, C.K. Nanoparticle–Cell Interactions: Molecular Structure of the Protein Corona and Cellular Outcomes. *Acc. Chem. Res.* **2014**, *47*, 2651–2659. [[CrossRef](#)] [[PubMed](#)]
44. Mosquera, J.; García, I.; Henriksen-Lacey, M.; Martínez-Calvo, M.; Dhanjani, M.; Mascareñas, J.L.; Liz-Marzán, L.M. Reversible Control of Protein Corona Formation on Gold Nanoparticles Using Host–Guest Interactions. *ACS Nano* **2020**, *14*, 5382–5391. [[CrossRef](#)] [[PubMed](#)]
45. Ke, P.C.; Lin, S.; Parak, W.J.; Davis, T.P.; Caruso, F. A Decade of the Protein Corona. *ACS Nano* **2017**, *11*, 11773–11776. [[CrossRef](#)]
46. Vroman, L. Effect of Adsorbed Proteins on the Wettability of Hydrophilic and Hydrophobic Solids. *Nat. Cell Biol.* **1962**, *196*, 476–477. [[CrossRef](#)]
47. Saptarshi, S.R.; Duschl, A.; Lopata, A.L. Interaction of nanoparticles with proteins: Relation to bio-reactivity of the nanoparticle. *J. Nanobiotechnol.* **2013**, *11*, 26. [[CrossRef](#)]
48. Luo, Z.; Murello, A.; Wilkins, D.M.; Kovacic, F.; Kohlbrecher, J.; Radulescu, A.; Okur, H.I.; Ong, Q.K.; Roke, S.; Ceriotti, M.; et al. Determination and evaluation of the nonadditivity in wetting of molecularly heterogeneous surfaces. *Proc. Natl. Acad. Sci. USA* **2019**, *116*, 25516–25523. [[CrossRef](#)]
49. Boselli, L.; Polo, E.; Castagnola, V.; Dawson, K.A. Regimes of Biomolecular Ultrasmall Nanoparticle Interactions. *Angew. Chem. Int. Ed.* **2017**, *56*, 4215–4218. [[CrossRef](#)]
50. Walkey, C.D.; Olsen, J.B.; Song, F.; Liu, R.; Guo, H.; Olsen, D.W.H.; Cohen, Y.; Emili, A.; Chan, W.C.W. Protein Corona Fingerprinting Predicts the Cellular Interaction of Gold and Silver Nanoparticles. *ACS Nano* **2014**, *8*, 2439–2455. [[CrossRef](#)]
51. Saha, K.; Rahimi, M.; Yazdani, M.; Kim, S.T.; Moyano, D.F.; Hou, S.; Das, R.; Mout, R.; Rezaee, F.; Mahmoudi, M.; et al. Regulation of Macrophage Recognition through the Interplay of Nanoparticle Surface Functionality and Protein Corona. *ACS Nano* **2016**, *10*, 4421–4430. [[CrossRef](#)] [[PubMed](#)]
52. Suk, J.S.; Xu, Q.; Kim, N.; Hanes, J.; Ensign, L.M. PEGylation as a strategy for improving nanoparticle-based drug and gene delivery. *Adv. Drug Deliv. Rev.* **2016**, *99*, 28–51. [[CrossRef](#)] [[PubMed](#)]

53. Schöttler, S.; Landfester, K.; Mailänder, V. Controlling the Stealth Effect of Nanocarriers through Understanding the Protein Corona. *Angew. Chem. Int. Ed.* **2016**, *55*, 8806–8815. [[CrossRef](#)]
54. Louie, S.M.; Gorham, J.M.; McGivney, E.A.; Liu, J.; Gregory, K.B.; Hackley, V.A. Photochemical Transformations of Thiolated Polyethylene Glycol Coatings on Gold Nanoparticles. *Environ. Sci. Nano* **2016**, *3*, 1090–1102. [[CrossRef](#)]
55. Zhang, F.; Skoda, M.W.A.; Jacobs, R.M.J.; Zorn, S.; Martin, R.A.; Martin, C.M.; Clark, G.F.; Goerigk, G.; Schreiber, F.; Goerigk, G. Gold Nanoparticles Decorated with Oligo(ethylene glycol) Thiols: Protein Resistance and Colloidal Stability†. *J. Phys. Chem. A* **2007**, *111*, 12229–12237. [[CrossRef](#)] [[PubMed](#)]
56. Schollbach, M.; Zhang, F.; Roosen-Runge, F.; Skoda, M.W.; Jacobs, R.M.; Schreiber, F. Gold nanoparticles decorated with oligo(ethylene glycol) thiols: Surface charges and interactions with proteins in solution. *J. Colloid Interface Sci.* **2014**, *426*, 31–38. [[CrossRef](#)]
57. Gunawan, C.; Lim, M.; Marquis, C.P.; Amal, R. Nanoparticle–protein corona complexes govern the biological fates and functions of nanoparticles. *J. Mater. Chem. B* **2014**, *2*, 2060–2083. [[CrossRef](#)] [[PubMed](#)]
58. Saha, K.; Moyano, D.F.; Rotello, V.M. Protein coronas suppress the hemolytic activity of hydrophilic and hydrophobic nanoparticles. *Mater. Horiz.* **2014**, *1*, 102–105. [[CrossRef](#)] [[PubMed](#)]
59. Riley, K.R.; Sims, C.M.; Wood, I.T.; Vanderah, D.J.; Walker, M.L. Short-chained oligo(ethylene oxide)-functionalized gold nanoparticles: Realization of significant protein resistance. *Anal. Bioanal. Chem.* **2017**, *410*, 145–154. [[CrossRef](#)] [[PubMed](#)]
60. Barbalinardo, M.; Caicci, F.; Cavallini, M.; Gentili, D. Protein Corona Mediated Uptake and Cytotoxicity of Silver Nanoparticles in Mouse Embryonic Fibroblast. *Small* **2018**, *14*, e1801219. [[CrossRef](#)]
61. García, K.P.; Zarschler, K.; Barbaro, L.; Barreto, J.A.; O'Malley, W.; Spiccia, L.; Stephan, H.; Graham, B. Zwitterionic-Coated “Stealth” Nanoparticles for Biomedical Applications: Recent Advances in Countering Biomolecular Corona Formation and Uptake by the Mononuclear Phagocyte System. *Small* **2014**, *10*, 2516–2529. [[CrossRef](#)] [[PubMed](#)]
62. Xiong, Z.; Shen, M.; Shi, X. Zwitterionic Modification of Nanomaterials for Improved Diagnosis of Cancer Cells. *BioConjug. Chem.* **2019**, *30*, 2519–2527. [[CrossRef](#)] [[PubMed](#)]
63. Choi, H.S.; Liu, W.; Liu, F.; Nasr, K.; Misra, P.; Bawendi, M.G.; Frangioni, J.V. Design considerations for tumour-targeted nanoparticles. *Nat. Nanotechnol.* **2009**, *5*, 42–47. [[CrossRef](#)]
64. Safavi-Sohi, R.; Maghari, S.; Raoufi, M.; Jalali, S.A.; Hajipour, M.J.; Ghassempour, A.; Mahmoudi, M. Bypassing Protein Corona Issue on Active Targeting: Zwitterionic Coatings Dictate Specific Interactions of Targeting Moieties and Cell Receptors. *ACS Appl. Mater. Interfaces* **2016**, *8*, 22808–22818. [[CrossRef](#)]
65. Loiola, L.M.; Batista, M.; Capeletti, L.B.; Mondo, G.B.; Rosa, R.S.; Marques, R.E.; Bajgelman, M.C.; Cardoso, M.B. Shielding and stealth effects of zwitterion moieties in double-functionalized silica nanoparticles. *J. Colloid Interface Sci.* **2019**, *553*, 540–548. [[CrossRef](#)]
66. Moyano, D.F.; Saha, K.; Prakash, G.; Yan, B.; Kong, H.; Yazdani, M.; Rotello, V.M. Fabrication of Corona-Free Nanoparticles with Tunable Hydrophobicity. *ACS Nano* **2014**, *8*, 6748–6755. [[CrossRef](#)]
67. Ashraf, S.; Park, J.; Bichelberger, M.A.; Kantner, K.; Hartmann, R.; Maffre, P.; Said, A.H.; Feliu, N.; Lee, J.; Lee, D.; et al. Zwitterionic surface coating of quantum dots reduces protein adsorption and cellular uptake. *Nanoscale* **2016**, *8*, 17794–17800. [[CrossRef](#)]
68. Zhang, X.; Liu, Y.; Gopalakrishnan, S.; Castellanos-Garcia, L.; Li, G.; Malassiné, M.; Uddin, I.; Huang, R.; Luther, D.C.; Vachet, R.W.; et al. Intracellular Activation of Bioorthogonal Nanozymes through Endosomal Proteolysis of the Protein Corona. *ACS Nano* **2020**, *14*, 4767–4773. [[CrossRef](#)]
69. Zhang, X.; Huang, R.; Gopalakrishnan, S.; Cao-Milán, R.; Rotello, V.M. Bioorthogonal Nanozymes: Progress towards Therapeutic Applications. *Trends Chem.* **2019**, *1*, 90–98. [[CrossRef](#)]
70. Cao-Milán, R.; Gopalakrishnan, S.; He, L.D.; Huang, R.; Wang, L.-S.; Castellanos, L.; Luther, D.C.; Landis, R.F.; Makabenta, J.M.V.; Li, C.-H.; et al. Thermally Gated Bio-orthogonal Nanozymes with Supramolecularly Confined Porphyrin Catalysts for Antimicrobial Uses. *Chem* **2020**, *6*, 1113–1124. [[CrossRef](#)]
71. Zhang, X.; Fedeli, S.; Gopalakrishnan, S.; Huang, R.; Gupta, A.; Luther, D.C.; Rotello, V.M. Protection and Isolation of Bioorthogonal Metal Catalysts by Using Monolayer-Coated Nanozymes. *ChemBioChem* **2020**, *21*, 2759–2763. [[CrossRef](#)] [[PubMed](#)]
72. Li, C.-H.; Huang, R.; Makabenta, J.M.; Schmidt-Malan, S.; Patel, R.; Rotello, V.M. In situ Generation of Antibiotics using Bioorthogonal “Nanofactories”. *Microbiol. Insights* **2021**, *14*, 1178636121997121. [[CrossRef](#)]
73. Huang, Y.; Ren, J.; Qu, X. Nanozymes: Classification, Catalytic Mechanisms, Activity Regulation, and Applications. *Chem. Rev.* **2019**, *119*, 4357–4412. [[CrossRef](#)]
74. Wu, J.; Wang, X.; Wang, Q.; Lou, Z.; Li, S.; Zhu, Y.; Qin, L.; Wei, H. Nanomaterials with enzyme-like characteristics (nanozymes): Next-generation artificial enzymes (II). *Chem. Soc. Rev.* **2019**, *48*, 1004–1076. [[CrossRef](#)]
75. Das, R.; Landis, R.F.; Tonga, G.Y.; Cao-Milán, R.; Luther, D.C.; Rotello, V.M. Control of Intra- versus Extracellular Bioorthogonal Catalysis Using Surface-Engineered Nanozymes. *ACS Nano* **2019**, *13*, 229–235. [[CrossRef](#)]
76. Doane, T.; Burda, C. Nanoparticle Mediated Non-Covalent Drug Delivery. *Adv. Drug Deliv. Rev.* **2013**, *65*, 607–621. [[CrossRef](#)]
77. Cho, E.C.; Xie, J.; Wurm, P.A.; Xia, Y. Understanding the Role of Surface Charges in Cellular Adsorption versus Internalization by Selectively Removing Gold Nanoparticles on the Cell Surface with a I2/KI Etchant. *Nano Lett.* **2009**, *9*, 1080–1084. [[CrossRef](#)]
78. Wilhelm, C.; Billotey, C.; Roger, J.; Pons, J.; Bacri, J.-C.; Gazeau, F. Intracellular uptake of anionic superparamagnetic nanoparticles as a function of their surface coating. *Biomaterials* **2003**, *24*, 1001–1011. [[CrossRef](#)]

79. Verma, A.; Stellacci, F. Effect of Surface Properties on Nanoparticle–Cell Interactions. *Small* **2010**, *6*, 12–21. [[CrossRef](#)] [[PubMed](#)]
80. Villanueva, A.; Cañete, M.; Roca, A.G.; Calero, M.; Veintemillas-Verdaguer, S.; Serna, C.J.; Morales, M.D.P.; Miranda, R. The influence of surface functionalization on the enhanced internalization of magnetic nanoparticles in cancer cells. *Nanotechnology* **2009**, *20*, 115103. [[CrossRef](#)] [[PubMed](#)]
81. Arvizo, R.R.; Miranda, O.R.; Thompson, M.A.; Pabelick, C.M.; Bhattacharya, R.; Robertson, J.D.; Rotello, V.M.; Prakash, Y.S.; Mukherjee, P. Effect of Nanoparticle Surface Charge at the Plasma Membrane and Beyond. *Nano Lett.* **2010**, *10*, 2543–2548. [[CrossRef](#)] [[PubMed](#)]
82. Kim, C.K.; Ghosh, P.; Pagliuca, C.; Zhu, Z.-J.; Menichetti, S.; Rotello, V.M. Entrapment of Hydrophobic Drugs in Nanoparticle Monolayers with Efficient Release into Cancer Cells. *J. Am. Chem. Soc.* **2009**, *131*, 1360–1361. [[CrossRef](#)] [[PubMed](#)]
83. Osaka, T.; Nakanishi, T.; Shanmugam, S.; Takahama, S.; Zhang, H. Effect of surface charge of magnetite nanoparticles on their internalization into breast cancer and umbilical vein endothelial cells. *Colloids Surf. B Biointerfaces* **2009**, *71*, 325–330. [[CrossRef](#)] [[PubMed](#)]
84. Farkhani, S.M.; Fard, A.A.; Zakeri-Milani, P.; Mojarrad, J.S.; Valizadeh, H. Enhancing antitumor activity of silver nanoparticles by modification with cell-penetrating peptides. *Artif. Cells Nanomed. Biotechnol.* **2017**, *45*, 1029–1035. [[CrossRef](#)]
85. Lim, S.; Kim, W.; Song, S.; Shim, M.K.; Yoon, H.Y.; Kim, B.-S.; Kwon, I.C.; Kim, K. Intracellular Uptake Mechanism of Bioorthogonally Conjugated Nanoparticles on Metabolically Engineered Mesenchymal Stem Cells. *BioConjug. Chem.* **2021**, *32*, 199–214. [[CrossRef](#)]
86. Hauck, T.S.; Ghazani, A.A.; Chan, W.C.W. Assessing the Effect of Surface Chemistry on Gold Nanorod Uptake, Toxicity, and Gene Expression in Mammalian Cells. *Small* **2008**, *4*, 153–159. [[CrossRef](#)]
87. Liu, X.L.; Wang, Y.T.; Ng, C.T.; Wang, R.; Jing, G.Y.; Yi, J.B.; Yang, J.; Bay, B.H.; Yung, L.-Y.L.; Di Fan, D.; et al. Coating Engineering of MnFe<sub>2</sub>O<sub>4</sub> Nanoparticles with Superhigh T<sub>2</sub> Relaxivity and Efficient Cellular Uptake for Highly Sensitive Magnetic Resonance Imaging. *Adv. Mater. Interfaces* **2014**, *1*, 1300069. [[CrossRef](#)]
88. Niikura, K.; Kobayashi, K.; Takeuchi, C.; Fujitani, N.; Takahara, S.; Ninomiya, T.; Hagiwara, K.; Mitomo, H.; Ito, Y.; Osada, Y.; et al. Amphiphilic Gold Nanoparticles Displaying Flexible Bifurcated Ligands as a Carrier for siRNA Delivery into the Cell Cytosol. *ACS Appl. Mater. Interfaces* **2014**, *6*, 22146–22154. [[CrossRef](#)]
89. Zhu, Z.-J.; Ghosh, P.S.; Miranda, O.R.; Vachet, R.W.; Rotello, V.M. Multiplexed Screening of Cellular Uptake of Gold Nanoparticles Using Laser Desorption/Ionization Mass Spectrometry. *J. Am. Chem. Soc.* **2008**, *130*, 14139–14143. [[CrossRef](#)]
90. Porret, E.; Sancey, L.; Martín-Serrano, A.; Montañez, M.I.; Seeman, R.; Yahia-Ammar, A.; Okuno, H.; Gomez, F.; Ariza, A.; Hildebrandt, N.; et al. Hydrophobicity of Gold Nanoclusters Influences Their Interactions with Biological Barriers. *Chem. Mater.* **2017**, *29*, 7497–7506. [[CrossRef](#)]
91. Sun, S.; Huang, Y.; Zhou, C.; Chen, S.; Yu, M.; Liu, J.; Zheng, J. Effect of Hydrophobicity on Nano-Bio Interactions of Zwitterionic Luminescent Gold Nanoparticles at the Cellular Level. *BioConjug. Chem.* **2018**, *29*, 1841–1846. [[CrossRef](#)] [[PubMed](#)]
92. Xuan, Y.; Zhang, R.-Y.; Zhao, D.-H.; Zhang, X.-S.; An, J.; Cheng, K.; Hou, X.-L.; Song, X.-L.; Zhao, Y.-D.; Yang, X.-Q. Ultrafast synthesis of gold nanosphere cluster coated by graphene quantum dot for active targeting PA/CT imaging and near-infrared laser/pH-triggered chemo-photothermal synergistic tumor therapy. *Chem. Eng. J.* **2019**, *369*, 87–99. [[CrossRef](#)]
93. Yu, S.; Mulero, M.C.; Chen, W.; Shang, X.; Tian, S.; Watanabe, J.; Watanabe, A.; Vorberg, T.; Wong, C.; Gately, D.; et al. Therapeutic Targeting of Tumor Cells Rich in LGR Stem Cell Receptors. *BioConjug. Chem.* **2021**, *32*, 376–384. [[CrossRef](#)]
94. Byrne, J.D.; Betancourt, T.; Brannon-Peppas, L. Active targeting schemes for nanoparticle systems in cancer therapeutics. *Adv. Drug Deliv. Rev.* **2008**, *60*, 1615–1626. [[CrossRef](#)] [[PubMed](#)]
95. Argudo, P.G.; Carril, M.; Martín-Romero, M.T.; Giner-Casares, J.J.; Carrillo-Carrión, C. Surface-Active Fluorinated Quantum Dots for Enhanced Cellular Uptake. *Chem. A Eur. J.* **2019**, *25*, 195–199. [[CrossRef](#)]
96. Marson, D.; Guida, F.; Şologan, M.; Boccardo, S.; Pengo, P.; Perissinotto, F.; Iacuzzi, V.; Pellizzoni, E.; Polizzi, S.; Casalis, L.; et al. Mixed Fluorinated/Hydrogenated Self-Assembled Monolayer-Protected Gold Nanoparticles: In Silico and In Vitro Behavior. *Small* **2019**, *15*, e1900323. [[CrossRef](#)]
97. Eskandari, Z.; Bahadori, F.; Celik, B.; Onyüksel, H. Targeted Nanomedicines for Cancer Therapy, From Basics to Clinical Trials. *J. Pharm. Pharm. Sci.* **2020**, *23*, 132–157. [[CrossRef](#)]
98. Werner, M.E.; Karve, S.; Sukumar, R.; Cummings, N.D.; Copp, J.A.; Chen, R.C.; Zhang, T.; Wang, A.Z. Folate-targeted nanoparticle delivery of chemo- and radiotherapeutics for the treatment of ovarian cancer peritoneal metastasis. *Biomaterials* **2011**, *32*, 8548–8554. [[CrossRef](#)]
99. Nogueira, E.; Gomes, A.C.; Preto, A.; Cavaco-Paulo, A. Folate-targeted nanoparticles for rheumatoid arthritis therapy. *Nanomed. Nanotechnol. Biol. Med.* **2016**, *12*, 1113–1126. [[CrossRef](#)]
100. Wilhelm, S.; Tavares, A.J.; Dai, Q.; Ohta, S.; Audet, J.; Dvorak, H.F.; Chan, W.C.W. Analysis of nanoparticle delivery to tumours. *Nat. Rev. Mater.* **2016**, *1*, 16014. [[CrossRef](#)]
101. Li, Y.; Wang, S.; Song, F.X.; Zhang, L.; Yang, W.; Wang, H.X.; Chen, Q.L. A pH-sensitive drug delivery system based on folic acid-targeted HBP-modified mesoporous silica nanoparticles for cancer therapy. *Colloids Surf. A Physicochem. Eng. Asp.* **2020**, *590*, 124470. [[CrossRef](#)]
102. Sudimack, J.; Lee, R.J. Targeted drug delivery via the folate receptor. *Adv. Drug Deliv. Rev.* **2000**, *41*, 147–162. [[CrossRef](#)]
103. Hartmann, L.C.; Keeney, G.L.; Lingle, W.L.; Christianson, T.J.; Varghese, B.; Hillman, D.; Oberg, A.L.; Low, P.S. Folate receptor overexpression is associated with poor outcome in breast cancer. *Int. J. Cancer* **2007**, *121*, 938–942. [[CrossRef](#)] [[PubMed](#)]

104. Kohler, N.; Sun, C.; Wang, J.; Zhang, M. Methotrexate-Modified Superparamagnetic Nanoparticles and Their Intracellular Uptake into Human Cancer Cells. *Langmuir* **2005**, *21*, 8858–8864. [[CrossRef](#)] [[PubMed](#)]
105. Yücel, O.; Şengelen, A.; Emik, S.; Önay-Uçar, E.; Arda, N.; Gürdağ, G. Folic acid-modified methotrexate-conjugated gold nanoparticles as nano-sized trojans for drug delivery to folate receptor-positive cancer cells. *Nanotechnology* **2020**, *31*, 355101. [[CrossRef](#)]
106. Cheng, W.; Nie, J.; Xu, L.; Liang, C.; Peng, Y.; Liu, G.; Wang, T.; Yunmei, P.; Huang, L.; Zeng, X. pH-Sensitive Delivery Vehicle Based on Folic Acid-Conjugated Polydopamine-Modified Mesoporous Silica Nanoparticles for Targeted Cancer Therapy. *ACS Appl. Mater. Interfaces* **2017**, *9*, 18462–18473. [[CrossRef](#)]
107. Kim, F.J.; Maher, C.M. Sigma1 Pharmacology in the Context of Cancer. *Snake Venoms* **2017**, *244*, 237–308. [[CrossRef](#)]
108. Rousseaux, C.G.; Greene, S.F. Sigma receptors [ $\sigma$ Rs]: Biology in normal and diseased states. *J. Recept. Signal Transduct.* **2015**, *36*, 1–62. [[CrossRef](#)] [[PubMed](#)]
109. Fitzgerald, K.A.; Rahme, K.; Guo, J.; Holmes, J.D.; O'Driscoll, C.M. Anisamide-targeted gold nanoparticles for siRNA delivery in prostate cancer—Synthesis, physicochemical characterisation and in vitro evaluation. *J. Mater. Chem. B* **2016**, *4*, 2242–2252. [[CrossRef](#)]
110. Luan, X.; Rahme, K.; Cong, Z.; Wang, L.; Zou, Y.; He, Y.; Yang, H.; Holmes, J.D.; O'Driscoll, C.M.; Guo, J. Anisamide-targeted PEGylated gold nanoparticles designed to target prostate cancer mediate: Enhanced systemic exposure of siRNA, tumour growth suppression and a synergistic therapeutic response in combination with paclitaxel in mice. *Eur. J. Pharm. Biopharm.* **2019**, *137*, 56–67. [[CrossRef](#)]
111. Purushothaman, B.; Choi, J.; Park, S.; Lee, J.; Samson, A.A.S.; Hong, S.; Song, J.M. Biotin-conjugated PEGylated porphyrin self-assembled nanoparticles co-targeting mitochondria and lysosomes for advanced chemo-photodynamic combination therapy. *J. Mater. Chem. B* **2018**, *7*, 65–79. [[CrossRef](#)]
112. Chen, P.; Zhang, X.; Venosa, A.; Lee, I.H.; Myers, D.; Holloway, J.A.; Prud'Homme, R.K.; Gao, D.; Szekely, Z.; Laskin, J.D.; et al. A Novel Bivalent Mannosylated Targeting Ligand Displayed on Nanoparticles Selectively Targets Anti-Inflammatory M2 Macrophages. *Pharmaceutics* **2020**, *12*, 243. [[CrossRef](#)]
113. Patil, T.S.; Deshpande, A.S. Mannosylated nanocarriers mediated site-specific drug delivery for the treatment of cancer and other infectious diseases: A state of the art review. *J. Control. Release* **2020**, *320*, 239–252. [[CrossRef](#)] [[PubMed](#)]
114. Li, J.; Li, M.; Tian, L.; Qiu, Y.; Yu, Q.; Wang, X.; Guo, R.; He, Q. Facile strategy by hyaluronic acid functional carbon dot-doxorubicin nanoparticles for CD44 targeted drug delivery and enhanced breast cancer therapy. *Int. J. Pharm.* **2020**, *578*, 119122. [[CrossRef](#)] [[PubMed](#)]
115. Chen, C.; Tang, W.; Jiang, D.; Yang, G.; Wang, X.; Zhou, L.; Zhang, W.; Wang, P. Hyaluronic acid conjugated polydopamine functionalized mesoporous silica nanoparticles for synergistic targeted chemo-photothermal therapy. *Nanoscale* **2019**, *11*, 11012–11024. [[CrossRef](#)] [[PubMed](#)]
116. Sykes, E.A.; Chen, J.; Zheng, G.; Chan, W.C. Investigating the Impact of Nanoparticle Size on Active and Passive Tumor Targeting Efficiency. *ACS Nano* **2014**, *8*, 5696–5706. [[CrossRef](#)]
117. Dai, Q.; Wilhelm, S.; Ding, D.; Syed, A.M.; Sindhvani, S.; Zhang, Y.; Chen, Y.Y.; Macmillan, P.; Chan, W.C.W. Quantifying the Ligand-Coated Nanoparticle Delivery to Cancer Cells in Solid Tumors. *ACS Nano* **2018**, *12*, 8423–8435. [[CrossRef](#)]
118. Du, J.; Lane, L.A.; Nie, S. Stimuli-responsive nanoparticles for targeting the tumor microenvironment. *J. Control. Release* **2015**, *219*, 205–214. [[CrossRef](#)]
119. Mura, S.; Nicolas, J.; Couvreur, P. Stimuli-responsive nanocarriers for drug delivery. *Nat. Mater.* **2013**, *12*, 991–1003. [[CrossRef](#)]
120. Grzelczak, M.; Liz-Marzán, L.M.; Klajn, R. Stimuli-responsive self-assembly of nanoparticles. *Chem. Soc. Rev.* **2019**, *48*, 1342–1361. [[CrossRef](#)]
121. Larsen, E.K.U.; Nielsen, T.; Wittenborn, T.; Birkedal, H.; Vorup-Jensen, T.; Jakobsen, M.H.; Østergaard, L.; Horsman, M.R.; Besenbacher, F.; Howard, K.A.; et al. Size-Dependent Accumulation of PEGylated Silane-Coated Magnetic Iron Oxide Nanoparticles in Murine Tumors. *ACS Nano* **2009**, *3*, 1947–1951. [[CrossRef](#)]
122. Ruan, S.; Hu, C.; Tang, X.; Cun, X.; Xiao, W.; Shi, K.; He, Q.; Gao, H. Increased Gold Nanoparticle Retention in Brain Tumors by in Situ Enzyme-Induced Aggregation. *ACS Nano* **2016**, *10*, 10086–10098. [[CrossRef](#)]
123. Ruan, S.; Xiao, W.; Hu, C.; Zhang, H.; Rao, J.; Wang, S.; Wang, X.; He, Q.; Gao, H. Ligand-Mediated and Enzyme-Directed Precise Targeting and Retention for the Enhanced Treatment of Glioblastoma. *ACS Appl. Mater. Interfaces* **2017**, *9*, 20348–20360. [[CrossRef](#)]
124. Xiao, W.; Ruan, S.; Yu, W.; Wang, R.; Huile, G.; Liu, R.; Gao, H. Normalizing Tumor Vessels To Increase the Enzyme-Induced Retention and Targeting of Gold Nanoparticle for Breast Cancer Imaging and Treatment. *Mol. Pharm.* **2017**, *14*, 3489–3498. [[CrossRef](#)] [[PubMed](#)]
125. Huang, R.; Li, C.-H.; Cao-Milán, R.; He, L.D.; Makabenta, J.M.; Zhang, X.; Yu, E.; Rotello, V.M. Polymer-Based Bioorthogonal Nanocatalysts for the Treatment of Bacterial Biofilms. *J. Am. Chem. Soc.* **2020**, *142*, 10723–10729. [[CrossRef](#)] [[PubMed](#)]
126. Wang, J.; Li, J.; Li, Y.; Zhang, Z.; Wang, L.; Wang, D.; Su, L.; Zhang, X.; Tang, B.Z. pH-Responsive Au(i)-disulfide nanoparticles with tunable aggregation-induced emission for monitoring intragastric acidity. *Chem. Sci.* **2020**, *11*, 6472–6478. [[CrossRef](#)]
127. Wu, W.; Luo, L.; Wang, Y.; Wu, Q.; Dai, H.-B.; Li, J.-S.; Durkan, C.; Wang, N.; Wang, G.-X. Endogenous pH-responsive nanoparticles with programmable size changes for targeted tumor therapy and imaging applications. *Theranostics* **2018**, *8*, 3038–3058. [[CrossRef](#)] [[PubMed](#)]

128. Park, S.; Lee, W.J.; Park, S.; Choi, D.; Kim, S.; Park, N. Reversibly pH-responsive gold nanoparticles and their applications for photothermal cancer therapy. *Sci. Rep.* **2019**, *9*, 1–9. [[CrossRef](#)]
129. Nam, J.; Won, N.; Jin, H.; Chung, H.; Kim, S. pH-Induced Aggregation of Gold Nanoparticles for Photothermal Cancer Therapy. *J. Am. Chem. Soc.* **2009**, *131*, 13639–13645. [[CrossRef](#)]
130. Song, J.; Kim, J.; Hwang, S.; Jeon, M.; Jeong, S.; Kim, C.; Kim, S. “Smart” gold nanoparticles for photoacoustic imaging: An imaging contrast agent responsive to the cancer microenvironment and signal amplification via pH-induced aggregation. *Chem. Commun.* **2016**, *52*, 8287–8290. [[CrossRef](#)]
131. Li, S.; Lui, K.-H.; Tsoi, T.H.; Lo, W.-S.; Li, X.; Hu, X.; Tai, W.C.-S.; Hung, C.H.-L.; Gu, Y.-J.; Wong, W.-T. pH-responsive targeted gold nanoparticles for in vivo photoacoustic imaging of tumor microenvironments. *Nanoscale Adv.* **2018**, *1*, 554–564. [[CrossRef](#)]
132. Hu, D.; Li, H.; Wang, B.; Ye, Z.; Lei, W.; Jia, F.; Jin, Q.; Ren, K.-F.; Ji, J. Surface-Adaptive Gold Nanoparticles with Effective Adherence and Enhanced Photothermal Ablation of Methicillin-Resistant *Staphylococcus aureus* Biofilm. *ACS Nano* **2017**, *11*, 9330–9339. [[CrossRef](#)] [[PubMed](#)]
133. Pillai, P.P.; Huda, S.; Kowalczyk, B.; Grzybowski, B.A. Controlled pH Stability and Adjustable Cellular Uptake of Mixed-Charge Nanoparticles. *J. Am. Chem. Soc.* **2013**, *135*, 6392–6395. [[CrossRef](#)] [[PubMed](#)]
134. Liu, X.; Chen, Y.; Li, H.; Huang, N.; Jin, Q.; Ren, K.; Ji, J. Enhanced Retention and Cellular Uptake of Nanoparticles in Tumors by Controlling Their Aggregation Behavior. *ACS Nano* **2013**, *7*, 6244–6257. [[CrossRef](#)] [[PubMed](#)]
135. Shen, Z.; Baker, W.; Ye, H.; Li, Y. pH-Dependent aggregation and pH-independent cell membrane adhesion of monolayer-protected mixed charged gold nanoparticles. *Nanoscale* **2019**, *11*, 7371–7385. [[CrossRef](#)] [[PubMed](#)]
136. Mizuhara, T.; Saha, K.; Moyano, D.F.; Kim, C.S.; Yan, B.; Kim, Y.-K.; Rotello, V.M. Acylsulfonamide-Functionalized Zwitterionic Gold Nanoparticles for Enhanced Cellular Uptake at Tumor pH. *Angew. Chem. Int. Ed.* **2015**, *54*, 6567–6570. [[CrossRef](#)] [[PubMed](#)]
137. Piao, J.-G.; Gao, F.; Li, Y.; Yu, L.; Liu, D.; Tan, Z.-B.; Xiong, Y.; Yang, L.; You, Y.-Z. pH-sensitive zwitterionic coating of gold nanocages improves tumor targeting and photothermal treatment efficacy. *Nano Res.* **2018**, *11*, 3193–3204. [[CrossRef](#)]
138. Gupta, A.; Das, R.; Tonga, G.Y.; Mizuhara, T.; Rotello, V.M. Charge-Switchable Nanozymes for Bioorthogonal Imaging of Biofilm-Associated Infections. *ACS Nano* **2018**, *12*, 89–94. [[CrossRef](#)]
139. Qiao, Z.; Yao, Y.; Song, S.; Yin, M.; Luo, J. Silver nanoparticles with pH induced surface charge switchable properties for antibacterial and antibiofilm applications. *J. Mater. Chem. B* **2018**, *7*, 830–840. [[CrossRef](#)]